Global joint inversion for the estimation of acoustic and shear impedances from AVO derived P- and S-wave reflectivity data

Xin-Quan Ma

Introduction

Although seismic inversion of post-stack data, estimating an acoustic impedance model, has become an almost routine procedure, the results can be of limited value due to the overwhelming problem of nonuniqueness in many cases of lithology and fluid discrimination. Variations in acoustic impedance may be due to any combination of a wide range of factors: lithology, porosity, fluid content and saturation, or pore pressure. In the last decade or so, there has been an increased interest in pre-stack inversion. This is because pre-stack inversion can generate not only compressional but also shear information about a rock. Therefore the use of two elastic parameters estimated from pre-stack inversion can have a significant impact in reducing the ambiguity in many exploration and development situations. For example, when gas is introduced into the pore space of a compressible brine-saturated sand, V_P drops, and V_S is slightly increased. These different behaviours of P- and S-waves when gas is present in the pore spaces make pre-stack inversion useful as a direct hydrocarbon indicator.

The most commonly used pre-stack inversion approaches to detecting lithology and fluid content have been to derive either *I* and *G* or *NI* and *PR* from pre-stack data, where *I* is AVO intercept, *G* is AVO gradient, *NI* is normal incidence reflectivity and *PR* is Poisson reflectivity. Cross-plotting these AVO attributes enables lithologies and fluid contents to be determined (Verm & Hilterman 1995). Smith & Gidlow (1987) showed that zero-offset P- and S-wave velocity reflectivity traces can be computed by least-squares fitting of an approximation of the Zoeppritz equations to the reflection amplitudes within a CMP gather. They combined these two reflectivity traces to obtain 'fluid factor' traces that can indicate the presence of gas. Fatti *et al.* (1994) also simplified the Zoeppritz equations to solve for zero-offset P- and S-wave reflection coefficients. Their formulation makes no assumption about V_S/V_P and about density, and is valid for incident angles of less than 50°. However these parameters derived from AVO equations are 'reflectivity' attributes, indicating changes in rock property at boundaries, rather than properties of layers. Furthermore, these data still contain wavelet effects and have impaired resolution. To understand rock properties for reservoir characterization, these reflectivity attributes must be inverted to reveal the rock properties rather than their changes at layer boundaries. Rock properties such as compressional- and shear-wave velocities, Poisson's ratio and acoustic and shear impedances are more readily tied to well logs, and are more directly related to reservoir properties. They are often direct hydrocarbon indicators and are also useful for mapping fluids within the reservoir and improving volumetric estimation (Pan *et al.* 1994; Castagna *et al.* 1995).

The accuracy and resolution of rock property estimates depend on which inversion algorithms are used. One of the most widely used algorithms is model-driven inversion. This algorithm is based on forwarding modelling of seismic data. Synthetic data are generated from an initial subsurface model and compared to the real seismic data; the model is modified and the synthetic data are updated and are compared to the real data again. If, after many iterations, no further improvement is achieved, the updated model is the inversion result. *A priori* information is usually incorporated in order to reduce the nonuniqueness of the output.

Within the model-driven inversion procedure, a misfit function is required to evaluate the quality of each trial model. Due to the highly band-limited nature of seismic data, the misfit function normally contains many local minima. We wish to find the lowest minimum by searching widely through the model space. This problem belongs to the category of global optimization. Global methods, usually using a Monte-Carlo random process, require no information on the derivatives of variables, and do not assume that the misfit function has a particular shape. Simulated annealing (SA) is one of the most widely used global methods, operating in analogy to thermodynamic systems. It is usually implemented by a 'drunkard's walk' through the model space, where steps

Correspondence: Scott Pickford Group Limited, 7th Floor, Leon House, 233 High Street, Croydon CR0 9XT, UK.

begin in random fashion, but are progressively biased towards the global minimum (Sen & Stoffa 1991; Goffe *et al.* 1994). Global methods in general avoid the limitations of local optimization methods and are particularly attractive in seismic waveform inversion.

In this paper, I describe a new method of joint inversion and show how both acoustic (P) and shear (S) impedances are inverted simultaneously using the simulated annealing approach. I also illustrate how the common nonuniqueness problem is reduced by constraining the algorithm using *a priori* low-frequency information. Both synthetic and field data examples are shown to demonstrate the validity of this new technique.

Global optimization by simulated annealing

Simulated annealing is a global optimization technique that mimics the physical process by which a crystal grows, by slow cooling of melt until the global minimum energy state is reached. It explores the objective function's surface and tries to optimize the function while moving both uphill and downhill. In simulated annealing, a random point in the model space is selected and the energy f or misfit is calculated. The new model is accepted unconditionally if the energy associated with the new point f' is lower ($\Delta f = f' - f < 0$). If the new point has a higher misfit ($\Delta f > 0$), then it is accepted with the probability $P = \exp(-\Delta f/T)$ where T is a control parameter called the acceptance temperature. The generation–acceptance process is repeated several times at a fixed temperature. Then the temperature is lowered following a cooling schedule and the process is repeated. The algorithm is stopped when the error does not change significantly after a sufficient number of trials. This acceptance criterion is known as the Metropolis rule (Metropolis *et al.* 1953). Since the probability of accepting a step in an uphill direction is always greater than zero, the algorithm can climb out of a local minimum. This is in contrast to the local search methods in which a new model is accepted only if $\Delta f < 0$, i.e. it always searches in the downhill direction (Cooke & Schneider 1983; Lines & Treitel 1984). Given a high starting temperature, simulated annealing first builds up a rough view of the objective function surface. When the temperature is decreased, the algorithm progresses to reduce the probability of accepting a bad step to zero as the global minimum is reached. More discussion on this subject and methods of determining this critical temperature can be found in Goffe *et al.* (1994) and Ma (2001).

A joint inversion scheme

An AVO analysis using the formulation of Fatti *et al.* (1994) generates zero-offset P- and S-wave reflectivity traces, both having the same two-way traveltime for a specific reflector, determined by the P-wave velocity. This analysis can be performed either on full CMP gathers, on partial offset gathers or on angle stacks. The more conventional AVO analysis using Shuey's formulation generates intercept (I) and gradient (G) sections. These I and G sections can also be converted into zero-offset P- and S-wave reflectivity sections, assuming that the relationship between P-wave velocity and density follows Gardner's rule (Bach *et al.* 1999). The P- and S-wave reflectivity sections, like post-stack seismic data, contain seismic wavelets and are indicative of rock-property changes across layer boundaries. In order to derive rock properties for each layer, an inversion of these data must be performed. A proper inversion should result in rock properties within layers and their changes with depth and in space. Here I propose a joint inversion scheme in which P- and S-impedances are parametrized together and solved simultaneously by a global optimization technique.

While the earth's impedance is a continuous function of depth, it is often advantageous to make a discrete approximation to this continuous function. When lithology boundaries are unknown, the earth model can be sampled as a number of microlayers of constant thickness and both layer interfaces and impedance need to be solved. If the total number of microlayers is larger than that of the true earth medium, this representation is defined as over-parametrization (Ma 2001). Another category is full-scale parametrization, by which the earth model is sampled at the same interval of equal two-way traveltime as in seismic data. This is the extreme case of over-parametrization requiring a large number of impedance unknowns, but no layer boundaries, to be solved. The full-scale parametrization scheme is discussed throughout this paper. Since P- and S-impedances are parametrized together, the number of parameters to be solved by the global optimization procedure is equal to the total number of samples in both P-wave and S-wave seismic traces.

Within the joint inversion scheme, model parameters are randomly perturbed, synthetic seismic data generated, and an objective function (misfit) calculated. The misfit is globally optimized by simulated annealing, which ensures that the global minimum, rather than a local minimum, is found. To reduce the nonuniqueness problem, the algorithm is constrained using *a priori* low-frequency information. The output is an earth model described by both acoustic (I_p) and shear (I_s) impedances at each sample interval. These impedance estimates can be used to derive rock properties such as Lamé's constants and Poisson's ratio, from which reservoir parameters can be estimated (Fig. 1).

Objective function and forward modelling

Optimization procedures require a misfit criterion (objective function) to evaluate the quality of each trial model. The optimum model is determined when the objective function is in the global minimum. An objective function may contain multiple terms, allowing different types of constraint to be built

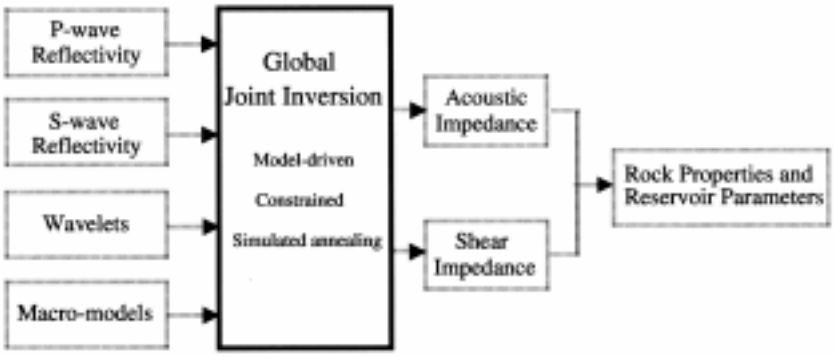

Figure 1 Global joint inversion work flow. The inputs to the inversion algorithm are P- and S-wave reflectivity series, P- and S-impedance macromodels and a wavelet. The outputs from the joint inversion are the optimized acoustic and shear impedances, which are then used to derive rock properties and reservoir parameters.

into the model. This is of crucial importance in reducing the nonuniqueness of inversion results. In seismic waveform inversion, the low-frequency impedance constraints are commonly used to reduce the nonuniqueness problem. In this paper, I use L_1-norm error functions. The first term is the least absolute deviation between the observed and modelled seismic trace. The second term consists of the misfit between *a priori* impedance and model impedance, which causes the solution to be close to the low-frequency impedance trend. The third term is the misfit between *a priori* V_S/V_P and model V_S/V_P (= I_S/I_P), which guides the search to follow the background lithology trend. The objective function is expressed as:

$$\Delta f = W_1\left(\frac{\sum_{i=1}^{n}\left|S_{\mathrm{P}\,\mathrm{obs}}{}^{i}-S_{\mathrm{P}\,\mathrm{mod}}{}^{i}\right|}{\sum_{i=1}^{n}\left|S_{\mathrm{P}\,\mathrm{obs}}{}^{i}\right|}+\frac{\sum_{i=1}^{n}\left|S_{\mathrm{S}\,\mathrm{obs}}{}^{i}-S_{\mathrm{S}\,\mathrm{mod}}{}^{i}\right|}{\sum_{i=1}^{n}\left|S_{\mathrm{S}\,\mathrm{obs}}{}^{i}\right|}\right)$$
$$+W_2\left(\frac{\sum_{i=1}^{n}\left|I_{\mathrm{P}\,\mathrm{pri}}{}^{i}-I_{\mathrm{P}\,\mathrm{mod}}{}^{i}\right|}{\sum_{i=1}^{n}\left|I_{\mathrm{P}\,\mathrm{pri}}{}^{i}\right|}+\frac{\sum_{i=1}^{n}\left|I_{\mathrm{S}\,\mathrm{pri}}{}^{i}-I_{\mathrm{S}\,\mathrm{mod}}{}^{i}\right|}{\sum_{i=1}^{n}\left|I_{\mathrm{S}\,\mathrm{pri}}{}^{i}\right|}\right)$$
$$+W_3\left(\frac{\sum_{i=1}^{n}\left|\left(I_{\mathrm{S}}{}^{i}/I_{\mathrm{P}}{}^{i}\right)_{\mathrm{pri}}-\left(I_{\mathrm{S}}{}^{i}/I_{\mathrm{P}}{}^{i}\right)_{\mathrm{mod}}\right|}{\sum_{i=1}^{n}\left|\left(I_{\mathrm{S}}{}^{i}/I_{\mathrm{P}}{}^{i}\right)_{\mathrm{pri}}\right|}\right), \qquad (1)$$

where $S_{\mathrm{P}\,\mathrm{obs}}{}^{i}$ and $S_{\mathrm{S}\,\mathrm{obs}}{}^{i}$ are P- and S-wave reflectivity traces derived from observed seismic gathers; $S_{\mathrm{P}\,\mathrm{mod}}{}^{i}$ and $S_{\mathrm{S}\,\mathrm{mod}}{}^{i}$ are synthetic P- and S-wave reflectivity traces generated by forward modelling; $I_{\mathrm{P}\,\mathrm{pri}}{}^{i}$ and $I_{\mathrm{S}\,\mathrm{pri}}{}^{i}$ are P- and S-impedance macromodels; $I_{\mathrm{P}\,\mathrm{mod}}{}^{i}$ and $I_{\mathrm{S}\,\mathrm{mod}}{}^{i}$ are modelled P- and S-impedances. Before inversion, both P and S seiemic amplitudes must be scaled to the level such that they match the synthetic seismic data generated from well logs. Since the three terms in the objective function have been normalized, the weighting factors can be chosen as $W_1 = W_2 = W_3 = 1$ in most cases. Note that there are $2n$ observation points, consisting of n P-wave reflectivity samples and n S-wave reflectivity samples. The number of parameters to be solved by the global optimization is also $2n$; the parameter vector consists of n P-impedance samples followed by n S-impedance samples.

To apply optimization algorithms to the inversion problem, a model must be found to generate synthetic seismograms so that a misfit between the observed and synthetic can be determined. In laterally homogeneous acoustic media, seismic propagation can be approximately modelled by the convolution theory:

$$S(t) = \int_{-\infty}^{\infty} R(\tau)\,W(t-\tau)\,\mathrm{d}\tau, \qquad (2)$$

where $S(t)$ is a seismic trace as a function of two-way traveltime, $W(t)$ is the seismic wavelet and $R(t)$ is the reflection coefficients series. The seismic source wavelet is usually unknown, but can be estimated using various techniques, for example, the partial coherence method of White (1980). This convolutional model establishes a relationship between the post-stack seismic data and the unknown model parameters such as velocity, density and impedance. However, a proper analysis of the seismic data must include the effects of geometrical divergence, anelastic absorption, dispersion of wavelet, transmission losses across the boundaries of the layered media, and multiple reflections. In this paper, these complications are ignored and I assume that the appropriate corrections have been applied.

When estimating a wavelet, we assume that the seismic trace is equivalent to the earth reflectivity convolved with a stationary wavelet plus some noise. The well data give us the earth reflectivity at the well locations. We have seismic data at these locations, and comparing a synthetic trace with seismic data will yield an estimate of the wavelet. The wavelet is the matching filter between the log and seismic segments and is computed using the auto-, cross- and power spectra of both

segments (White 1980). This method also quantifies the quality of match between the synthetic seismogram and the data, and hence indicates the validity of the convolutional model. A P-wave wavelet can be estimated using P-seismic data and the acoustic impedance log and an S-wave wavelet by S-seismic data and the shear impedance log. Both types of wavelet should be similar as both P-seismic and S-seismic data are derived from the same P-wave gather.

Constraints for uniqueness and stability

Seismic inversion is nonunique. This is true partly because measurements are incomplete and also because they involve uncertainties. In model-driven seismic inversion, the quality of a solution is determined by comparing the observed seismic trace to a synthetic trace generated from the solution. If these two are the same, then the solution is exact, but not necessarily unique. The impedance solution from seismic inversion is highly nonunique in the frequency ranges outside the bandwidth of the source wavelet. In the full-scale over-parametrized inversion scheme described in this paper, without appropriate constraints, the solution may exhibit strong, unstable oscillations; the algorithm may pick many contrasting impedance values within a homogeneous part of the model and consequently generates a poor match between the true and estimated impedances. To reduce the nonuniqueness and stabilize the solution, I apply the following constraints to the algorithm:

- *a priori* acoustic and shear impedance information, derived from well logs and seismic processing velocities, is used as a constraint expressed as a second term in the objective function (see Equation 1). This term along with the first misfit term has the effect of guiding the solution, moving towards the physically meaningful low-frequency trend. An *a priori* V_S/V_P 'lithology' constraint is added as a third term to guide the search to follow the background 'lithology' trend. These constraints are important in that they can compensate for the low-frequency components, which are missing in the band-limited seismic data, and also in that they allow absolute impedance values to be estimated for more accurate lithology and fluid identification.
- A search boundary is set up for each parameter, limiting the physical properties such that a set of possible solutions exists only within a defined corridor. The parameter bounds are derived directly from the low-frequency impedance trend. Both P-impedance and S-impedance boundaries are set up to constrain $2n$ model parameters. This constraint serves to speed up the convergence and hence to save computation time.
- Seismic amplitudes are used to modify the parameter search bounds and hence to reduce further the nonuniqueness problem and to stabilize the solution. This is based on the fact that layer boundaries with large impedance contrasts exhibit large amplitudes in seismic data. Therefore one should allow a wider search corridor for interfaces at which seismic amplitudes are large, and a narrower corridor for places where seismic amplitudes are

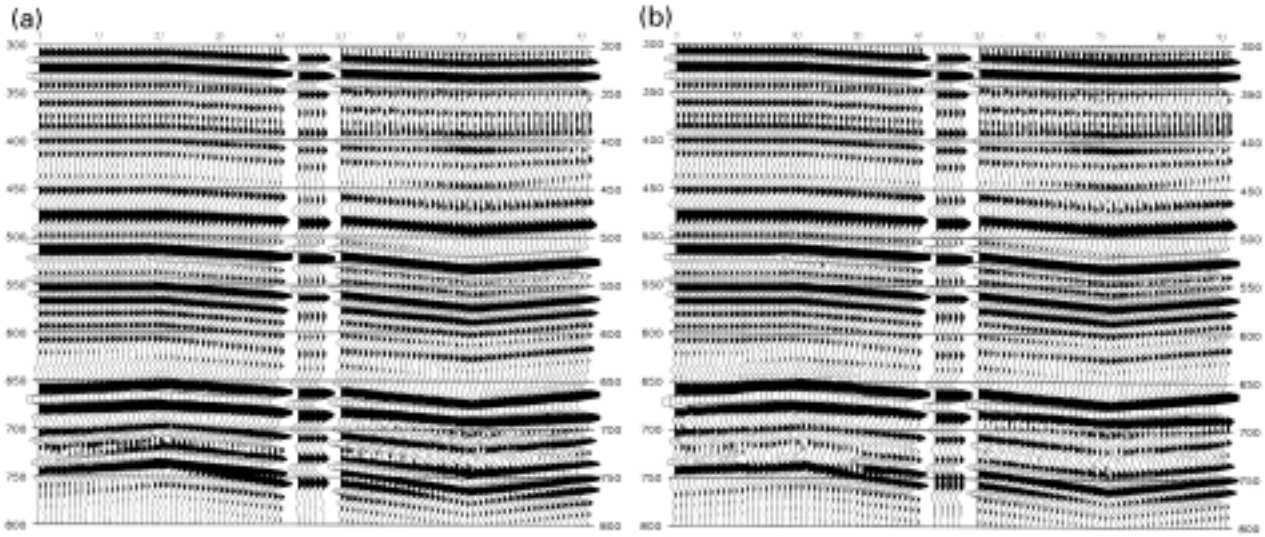

Figure 2 (a) Zero-offset P-wave reflectivity derived from pre-stack CMP gathers. While the gathers are generated using the exact Zoeppritz equations, the reflectivity traces are estimated by fitting Fatti's AVO equations against the gathers. The insert is the synthetic P-seismic trace calculated using the true acoustic impedance value, simulating a well tie, and used here to compare with the AVO extraction. (b) Zero-offset S-wave reflectivity derived from pre-stack CMP gathers. The insert is the synthetic S-seismic trace calculated using the true shear impedance trace. Note that the effect on the S-reflectivity image is evident at 660 ms and between CDPs 10–30, as a result of introducing a high V_S anomaly.

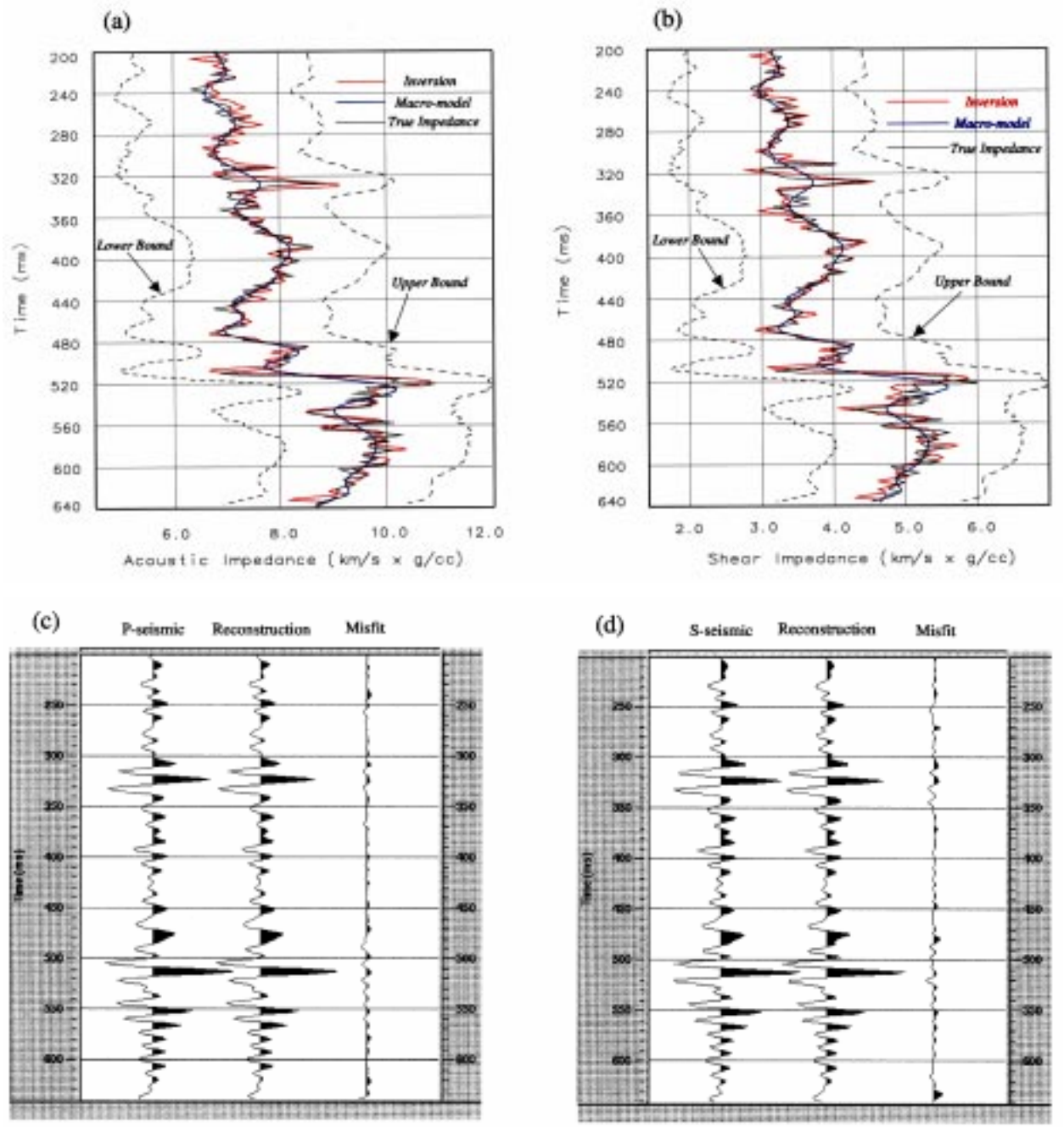

Figure 3 The global joint inversion is applied to a single pair of P- and S-seismic traces. The macromodels are obtained by smoothing the true impedance models. (a) Acoustic impedance solution. The starting model is the macromodel shown in blue. The lower bounds and upper bounds are defined using both the macromodel and seismic envelope. (b) Shear impedance solution. Note that the S-wave macromodel and search corridors are different from its P-wave counterparts, with S-impedance corridors being narrower than the P-impedance corridors. (c) P-seismic, its reconstruction from the inverted P-impedance trace and their misfits. (d) S-seismic, its reconstruction from the inverted S-impedance trace and their misfits.

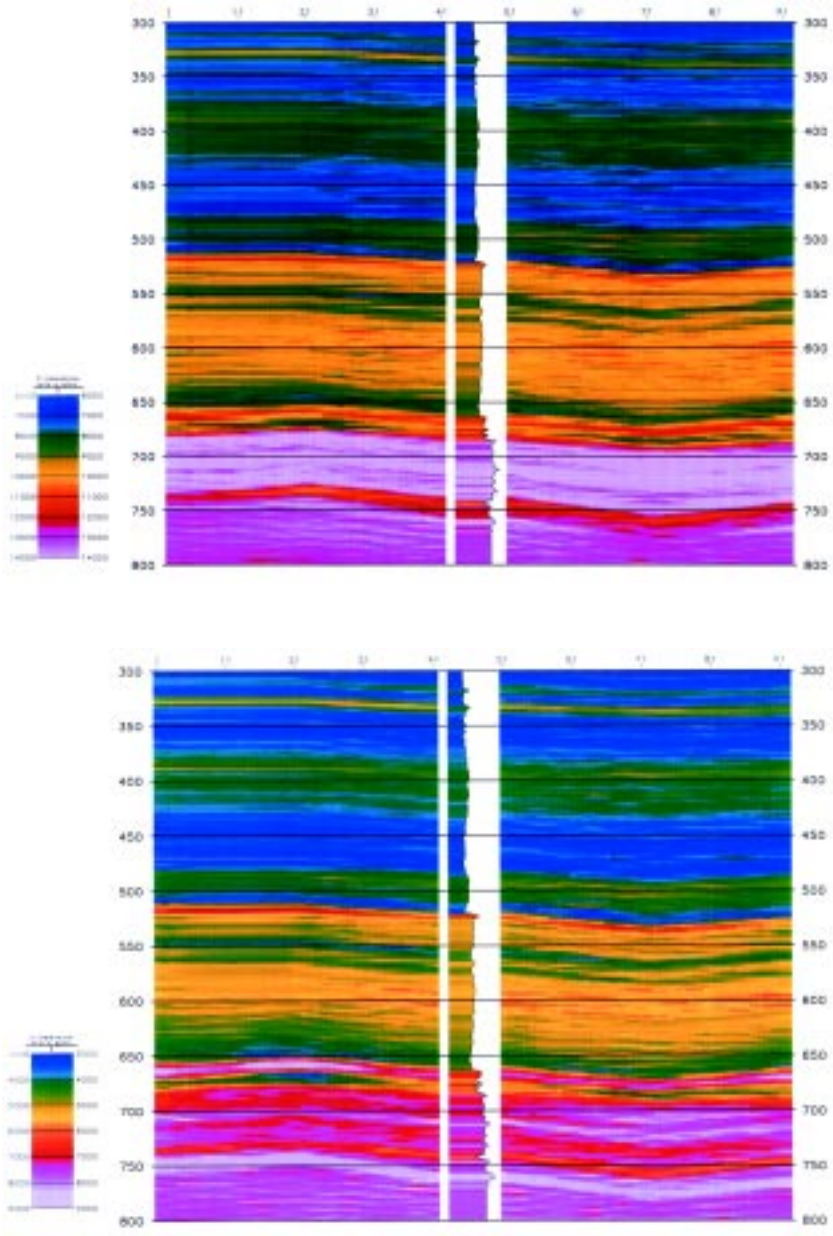

Figure 4 The global joint inversion from P- and S-seismic data shown in Fig. 2(a,b). (a) Acoustic impedance section shows a smooth lateral consistency and a high vertical resolution. The insert is the true acoustic impedance trace, simulating a well log, and shows a very good match with the inversion results. (b) Shear impedance output. The insert is the true shear impedance trace, and is also used for comparison with the inversion results. Note that a high shear impedance anomaly at 660 ms and between CDPs 10–30 is predicted from the joint inversion.

small. In practice, two RMS gain curves from P-wave and S-wave seismic traces are calculated and incorporated into the parameter search boundaries.

Synthetic data example.

Using eight sets of fictitious V_P, V_S and ρ well logs, and horizon-based interpolation, we construct a 2D geological earth model and generate a '2.5D' line of synthetic pre-stack gathers. The label '2.5D' refers to a mathematical formalism that acknowledges the 3D propagation characteristics of the wavefield, but seeks only a 2D description of the subsurface. The synthetic pre-stack gathers are generated using the Zoeppritz equations with ray tracing, which assumes a simple plane-wave approximation to the source signal propagating through our earth model.

From this set of modelled pre-stack data, we can extract pre-stack AVO attributes. We use the AVO equations of Fatti *et al.* (1994) to extract zero-offset P- and S-wave reflectivities. To accomplish this, we also need the background P-wave velocity to determine the incident angles by ray tracing and the V_S/V_P ratio as required by Fatti's AVO formula. P-reflectivities and S-reflectivities are then obtained through a

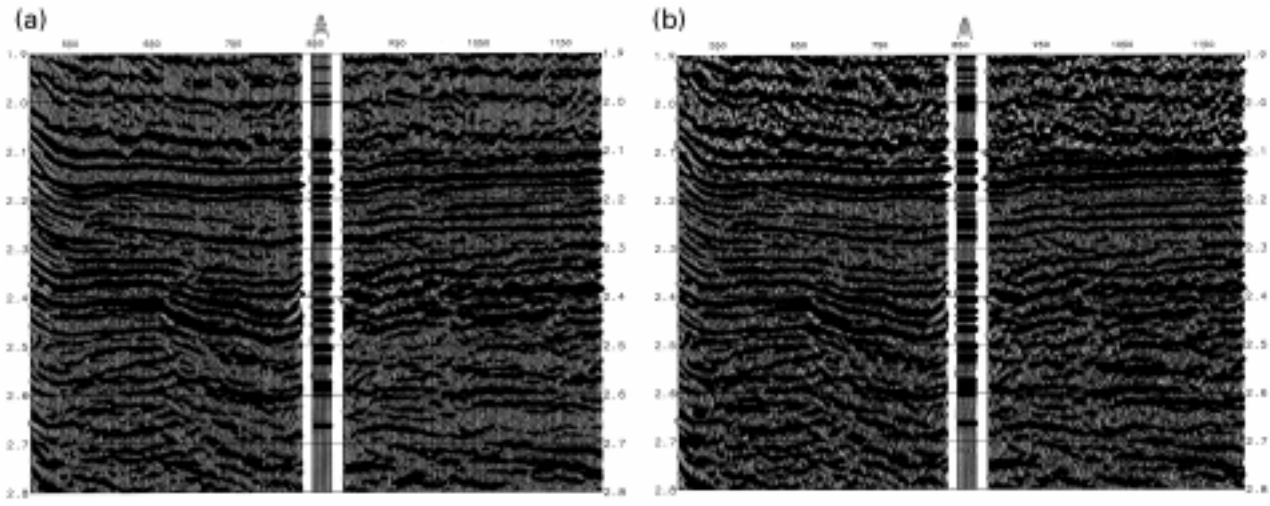

Figure 5 (a) Zero-offset P-wave reflectivity derived from pre-stack CMP gathers. The chalk sequence between 2150 and 2450 ms is the most prominent feature. The sand of interest is very close to the base of the Chalk. The insert shows P-seismic traces calculated using the log acoustic impedance trace, and plotted here for comparison with the AVO extraction. (b) Zero-offset S-wave reflectivity derived from pre-stack CMP gathers. The insert shows S-seismic traces calculated using the log shear impedance. The inserted logs show good correspondence with the reflectivity image.

least-squares fit to the modelled pre-stack gathers. The reflectivity series are shown in Fig. 2(a,b). Note that there is an anomaly in the S-wave reflectivity section at 660 ms and between CDPs 10–30. This is the result of inserting a layer of high shear-wave velocity at this depth. To compare the AVO-derived seismic with synthetic seismic, simulating a well tie, we calculate a synthetic seismic trace using the true reflection coefficients derived from true P- and S-impedance traces and a wavelet estimated from the AVO-derived seismic data. The synthetic seismic traces are plotted together with P- and S-reflectivity traces, showing a very good match between the two.

The global joint inversion approach is applied to the above data set to estimate acoustic and shear impedances. To accomplish this, one needs to supply the objective function, lower and upper parameter bounds, initial model parameters (or a starting model), initial annealing temperature and a stop criterion. For forward modelling, a wavelet is also required. The initial model is set to be the low-frequency impedance model, which has the same number of samples as the seismic data. The lower and upper bounds of impedance parameters are derived from the low-frequency impedance trend, subsequently modified by the seismic trace envelopes (Fig. 3a,b). Forward modelling is carried out for P- and S-seismic separately, and the results are then combined to form the objective function weighted against the impedance and V_S/V_P constraints. The simulated annealing algorithm begins by calculating the objective function using the initial model parameters and it then accepts or rejects this move using the Metropolis criterion. Many iterations are allowed to be performed at a given temperature. The temperature, T', is then lowered and the computation continues until the stop criterion is satisfied. The cooling scheme is given by $T' = rT$, where r is a temperature reduction factor set between 0 and 1, and T is the temperature in the previous computation loop (Ma 2001). The outputs are the optimized acoustic and shear impedance values.

To demonstrate the global joint inversion capabilities, I take the first trace from the P-reflectivity stack and the first trace from the S-reflectivity stack (see Fig. 2a,b) and perform a joint inversion of them. The results are shown in Fig. 3(a,b). The estimated P and S impedances match the true model well. Note that impedance corridors defining parameter perturbation windows are different from sample to sample. This is the result of incorporating seismic envelopes into the parameter bounds; a search corridor is wider for interfaces at which seismic amplitudes are large, and narrower in locations where seismic amplitudes are small. The synthetic seismic traces calculated using the inverted impedance profiles have been plotted along with the 'observed' traces. The misfit traces indicate that nearly all energy in the 'observed' traces has been inverted, resulting in almost zero error traces (Fig. 3c,d).

I then run the inversion for P- and S-reflectivity stacks (Fig. 2a,b). The estimated acoustic and shear impedances are shown in Fig. 4(a,b), respectively. Note that a layer with high

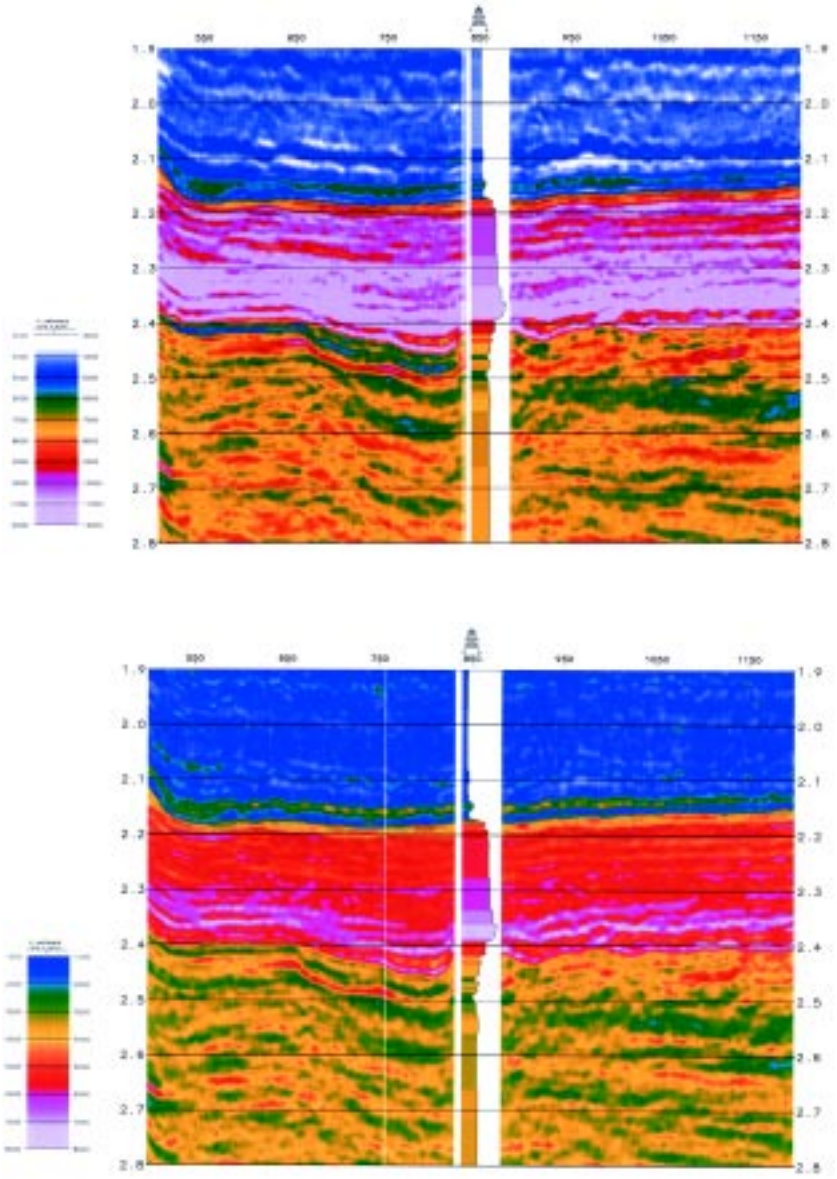

Figure 6 The global joint inversion of P and S-seismic data shown in Fig. 5(a,b). (a) Acoustic impedance solution. The insert is the log acoustic impedance trace showing a good match with the inversion results. (b) Shear impedance solution. The insert is the log shear impedance trace, and is also used for comparison with the inversion results.

shear impedance is well predicted at 660 ms and between CDPs 10–30. For comparison, I insert a true acoustic impedance trace and a true shear impedance trace into the impedance sections, simulating a log match. It can be seen that the inverted impedance matches well at this location, and that lateral variations of impedance values within layers are evident. Trace-to-trace continuity is very high, demonstrating the stability of the method.

Field data example

The pre-stack seismic data are from a North Sea 3D survey. A true-amplitude processing sequence was applied to the data, which preserves the offset-dependent reflectivity. The key ingredients in the processing sequence include predictive deconvolution, offset variant gain recovery, radon multiple attenuation and pre-stack 3D time migration. The gathers were NMO-corrected before the AVO analysis. There were three wells in the area, where P-wave and density logs were available. S-wave logs were derived from an empirical relationship between V_S and V_P, obtained from nearby wells. These logs, together with seismic horizons, were used to construct macro-velocity and impedance models for AVO analysis and for global joint inversion. The CMP gathers and smoothed P- and S-wave velocities were the inputs to the AVO analysis. The outputs of the AVO analysis are stacks of 'zero-offset P-wave' reflectivity series (Fig. 5a) and 'zero-offset S-wave' reflectivity series (Fig. 5b).

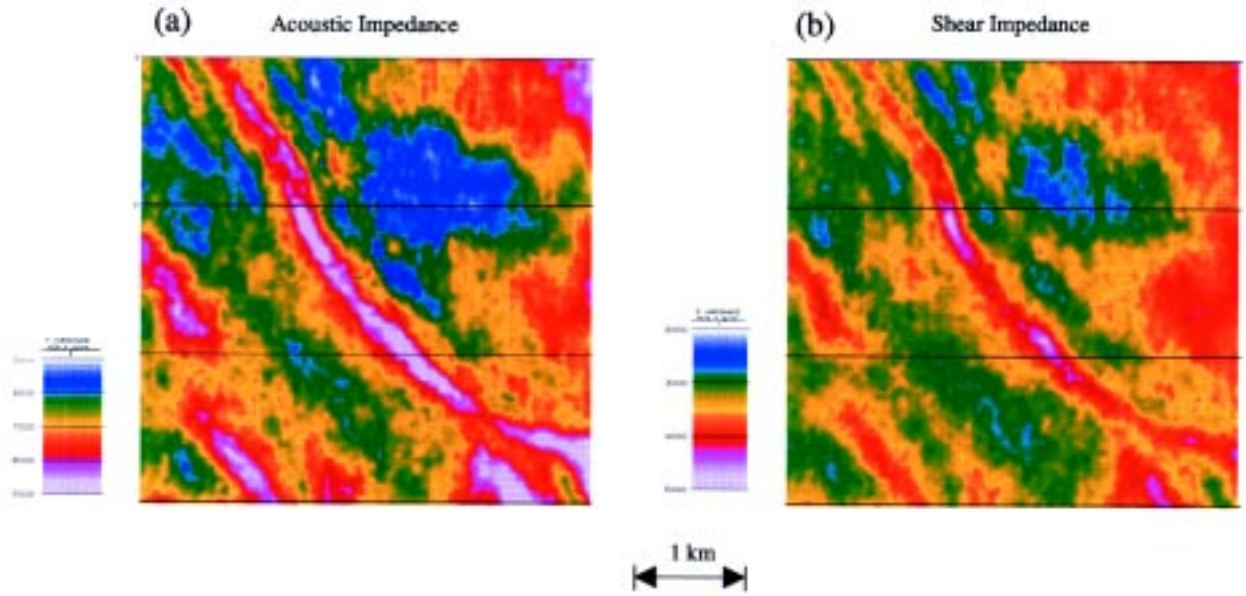

Figure 7 Time slices of (a) acoustic and (b) shear impedance volumes centred at a well location. The two-way traveltime of the slices is 2450 ms, just below the base of the Chalk. These two impedance volumes can be combined to generate rock properties, which enable the lithologies and fluid contents to be identified.

The low-frequency macromodel was generated using all the well data and the seismic horizon data. A velocity function of the form $V = V_0 + kZ$ was determined for each of the interpreted units between the horizons, where V_0 is the velocity at the horizontal surface datum. V is the velocity in m/s at a depth Z below the datum plane and k is a constant whose value is generally between 0.3 s^{-1} and 1.3 s^{-1} (Al-Chalabi 1997). This function was then interpolated for all CDP bins and for each of these a velocity trace in time was generated. The velocity volume was then converted to impedance using the interpolated density volume. The low-frequency shear impedance volume was created in a similar fashion.

The joint inversion algorithm takes five data sets as input; they are P- and S-seismic, and low frequency P- and S-impedances and a wavelet. It outputs both acoustic (I_P) and shear (I_S) impedance traces. Figure 6(a,b) show the inversion results for a seismic in-line crossing the well. It can be seen that the inverted P- and S- impedances show a high vertical resolution and a lateral consistency. The well match is also very good. Two time slices for the inverted acoustic and shear impedance volumes are shown in Fig. 7. These results can be combined to derive rock properties such as Poisson's ratio and Lamé's parameters for detection, identification and quantification of lithologies and fluid contents of reservoirs and potential reservoir targets.

Conclusions

1 The global joint inversion algorithm has been developed to estimate both acoustic and shear impedances simultaneously from AVO-derived P-wave and S-wave reflectivity data. The inversion procedure adopts a global optimization method of simulated annealing to locate a global minimum of a multivariable objective function. Constraints derived from low-frequency P- and S-impedance models and the background V_S/V_P ratio have been applied to the inversion algorithm, allowing the nonuniqueness problem to be reduced and much greater stability to be achieved. The full-scale parametrization scheme permits a high vertical resolution to be extracted for both acoustic and shear impedances.

2 Application of the global joint inversion method to synthetic and field examples has shown that it is capable of producing both acoustic and shear impedances with a high vertical resolution and a lateral consistency. These estimated impedance data can be used to derive rock properties such as Poisson's ratio and Lamé's parameters for discrimination between reservoir fluids and lithologies.

Acknowledgements

The author thanks Paul Haskey and Adrian Pelham from the Croydon office of the Scott Pickford Group for the stimulating discussion and for reading this manuscript, the staff from

the Calgary office of the Scott Pickford Group for providing the synthetic seismic data. The author is grateful to Techmarine International Ltd for providing the North Sea data.

References

Al-Chalabi, M. [1997] Parameter nonuniqueness in velocity versus depth functions. *Geophysics* **62**, 970–979.

Bach, T., Espersen, T.B., Hinkley, R., Pillet, W.R., Pedersen, J.M. and Rasmussen, K.B. [1999] Seismic inversion of AVO data. *61st EAGE Conference, Helsinki, Extended Abstracts*, paper 6-54.

Castagna, J.P., Batzle, M.L. and Kan, T.K. [1995] Rock physics – the link between rock properties and AVO response. In: *SEG Investigations in Geophysics,* Volume 8. *Offset-Dependent Reflectivity – Theory and Practice of AVO Analysis*. SEG, Tulsa, OK.

Cooke, D.A. and Schneider, W.A. [1983] Generalised linear inversion of reflection seismic data. *Geophysics* **48**, 665–676.

Fatti, J.L., Smith, G.C., Vail, P.J., Strauss, P.J. and Levitt, P.R. [1994] Detection of gas in sandstone reservoirs using AVO analysis: a 3D seismic case history using the Geostack technique. *Geophysics* **59**, 1362–1376.

Goffe, W.L., Ferrier, G.D. and Rogers, J. [1994] Global optimization of statistical functions with simulated annealing. *Journal of Econometrics* **60**, 65–100.

Lines, L.R. and Treitel, S. [1984] A review of least-squares inversion and its application to geophysical problems. *Geophysical Prospecting* **32**, 159–186.

Ma, X.Q. [2001] A constrained global inversion method using an over-parameterised scheme: application to poststack seismic data. *Geophysics* **66**, 613–626.

Metropolis, N., Rosenbluth, A., Rosenbluth, M., Teller, A. and Teller, E. [1953] Equation of state calculations by fast computing machines. *Journal of Chemical Physics* **21**, 1087–1092.

Pan, G.S., Young, C.Y. and Castagna, J.P. [1994] An integrated target-orientated prestack elastic waveform inversion: sensitivity, calibration, and application. *Geophysics* **59**, 1392–1404.

Sen, M.K. and Stoffa, P.L. [1991] Nonlinear one-dimensional seismic waveform inversion using simulated annealing. *Geophysics* **56**, 1624–1638.

Shuey, R.T. [1985] A simplification of the Zoeppritz equations. *Geophysics* **50**, 609–614.

Smith, G.C. and Gidlow, P.M. [1987] Weighted stacking for rock property estimation and detection of gas. *Geophysical Prospecting* **35**, 993–1014.

Verm, R. and Hilterman, F. [1995] Lithology color-coded seismic sections: The calibration of AVO crossplotting to rock properties. *Leading Edge* **14**, 847–853.

White, R.E. [1980] Partial coherence matching of synthetic seismograms with seismic traces. *Geophysical Prospecting* **28**, 333–358.